Topic: EX-D

Key dependencies for the radial density decay in the far-SOL of JET H-mode plasmas

C. Perez von Thun[1], R.B. Morales[2], M. Bernert[3], L. Frassinetti[4], N. Vianello[5], A. Huber[6], B. Lomanowski[7], A.G. Meigs[2], N. Panadero[8], G. Sergienko[6], S.A. Silburn[2], D. Silvagni[3], B. Thomas[2], A. Tookey[2], S. Aleiferis[9], A. Boboc[2], M. Brix[2], M. Faitsch[3], M. Groth[10], O. Grover[3], D. Kos[2], M. Lennholm[2], D. Refy[11], H.J. Sun[2], G. Szepesi[2], JET Contributors* and the EUROfusion Tokamak Exploitation Team**

*[1]Institute of Plasma Physics and Laser Microfusion, Hery 23, 01-497 Warsaw, Poland. [2]UKAEA, Culham Campus, Abingdon, OX14 3DB, UK. [3]Max-Planck-Institut für Plasmaphysik, D-85748 Garching, Germany. [4]Fusion Plasma Physics, KTH, Stockholm, Sweden. [5]Consorzio RFX, 35127 Padova, Italy. [6]Forschungszentrum Jülich GmbH, Institute of Fusion Energy and Nuclear Waste Management – Plasma Physics, Jülich, Germany. [7]Oak Ridge National Laboratory, Oak Ridge, TN 37831, USA. [8]Laboratorio Nacional de Fusión, CIEMAT, Madrid, Spain. [9]NCSR 'Demokritos', 153 10, Agia Paraskevi Attikis, Greece. [10]Aalto University, PO Box 14100, FIN-00076 Aalto, Finland. [11]Centre for Energy Research, POB 49, H-1525 Budapest, Hungary. *See the author list of "Overview of T and D-T results in JET with ITER-like wall" by CF Maggi et al. Nuclear Fusion 64 (2024) 112012, DOI: 10.1088/1741-4326/ad3e16. ** See the author list of "Overview of the EUROfusion Tokamak Exploitation programme in support of ITER and DEMO" by E. Joffrin Nuclear Fusion 2024 10.1088/1741-4326/ad2be4. E-mail:* christian.perez.von.thun@ifpilm.pl

With ITER now foreseen to operate in a full-W wall, and simulations suggesting the main chamber to be the dominant W source [1], advancing our physics understanding of density flattening in the far-SOL and the formation of density shoulders is critical [2]. In addition, to correctly predict how dense the far-SOL plasma in front of the main chamber tiles in ITER will be, it is crucial to understand the physics that sets the radius of the second (outer) inflection of the density shoulder [3] on the low field side (LFS), and whether it is possible to modify it by external means.

A dedicated H-mode fuelling ramp experiment was implemented on JET, designed to take advantage of improvements to the FM-CW reflectometer [4]. A highly diverse set of near- and far-SOL profiles was compiled, by ramping the density from medium- low values up to the H-L backtransition (H-mode density limit) for a variety of target plasmas. In conjunction with other edge diagnostics, these experiments have delivered inter-ELM main chamber SOL density information with unprecedented detail on JET.

The key results for the far-SOL on JET (for which we use $\psi_N > 1.025$) is summarised as follows:

High q_{cyl} (high connection length $L_{||}$ to the divertor) favours SOL density shoulder formation: repeating the same fuelling ramp at increased Ip =1.9MA (B_t fixed) yielded no shoulder formation up to the H-L backtransition (figure 1) despite achieving deep divertor detachment ($T_{e,OSP}$<1eV). A similar trend was reported on TCV and AUG, albeit in L-mode [5].

Divertor geometry is not found to play an important role: For fixed turbulence control parameter α_t (evaluated at ψ_N=1, assuming flat Zeff profile, and with Te at the separatrix determined via power balance including broadening of the near-SOL power width) [6], moving the outer strike point (OSP) from horizontal target (HT) to vertical target (VT) strongly impacted the density gradients for the pedestal and near-SOL, but not the radial density decay in the far-SOL (figures 2 and 3).

Secondly, the studies show that **$\lambda_{n,far}$ and $\lambda_{n,near}$ are independent** (e.g. figure 2) and uncorrelated (different physics involved), as reported previously [7]. Here, **$\lambda_{n,far}$** has been determined via exponential fitting in region $1.025 < \psi_N <\sim 1.07\text{-}1.08$.

Increased plasma triangularity enables access to higher absolute edge densities (both for pedestal and SOL), but the radial decay **$\lambda_{n,far}$ is not strongly affected** (figure 3)**.**

Switching from gas fuelling to pellet fuelling yields lower absolute SOL densities at fixed α_t, both in the near- and far SOL regions. However, most of this difference originates from the near-SOL (where find steeper slope with pellets than with gas), whereas **in the far-SOL the radial decay found is comparable with pellets or gas** (figure 3).

The overarching result of this work (figure 3) is that, in spite of the dataset's heterogeneity, **results are unified when using the turbulence control parameter α_t.** Since $\alpha_t \sim q_{cyl}^2$, the identification of α_t as the primary driver for SOL flattening also provides a direct explanation for the lack of density shoulder formation in the Ip=1.9MA case: the q_{cyl} reduction from 5.1 to 3.5 prevented α_t from exceeding unity, whereas all the 'SOL density shoulders' were found above $\alpha_t \geq \sim 1.1$. Thus, **α_t is found to be a good descriptor for quantifying far-SOL density flattening on JET.**

In figure 3, **a 'global' inverse proportionality for the radial decay constant ($1/\lambda_{n,far}$) ~ $\alpha_t^{-0.8}$ is found** (dashed line). However, the **possible presence of a $\lambda_{n,far}$ plateau** in the range α_t =0.7-1.0 cannot be excluded, above which $\lambda_{n,far}$ increases again -initially more sharply- and for $\alpha_t \geq 1.1$ enters the regime where 'density shoulders' are observed.

Earlier studies on AUG [8] found that the **second (outer) shoulder inflection radius** was set by the

intersection of flux surfaces with the LFS poloidal limiters (with the work in [3] also strongly suggesting toroidal non-uniformities are important). This is *not* the case for these JET density ramp experiments, which were run with higher than usual clearance to the LFS wall for operational reasons. Flux surface mapping results for density shoulders obtained with three different plasma shapes (figure 4) show that neither LFS poloidal limiters (too far out) nor the HFS inner wall guard limiter (too far in) coincide with the shoulder inflection radius. Instead, an **excellent correlation between the shoulder inflection radius and the intersection with the LFS divertor top** is found. A plausible explanation is that as the filaments drift towards the LFS, their bottom end will encounter hotter and less dense conditions near the divertor shoulder compared to the cold and dense divertor and this might enable electrical reconnection. This important finding may provide a relatively simple route (through careful equilibrium design) to prevent direct contact of a density shoulder in ITER with the main chamber walls and drastically reduce the W source.

In conclusion, **these results offer a promising physics route for extrapolation from current day machines to ITER, and to constrain with sufficient accuracy modelling predictions for the W source expected in ITER.**

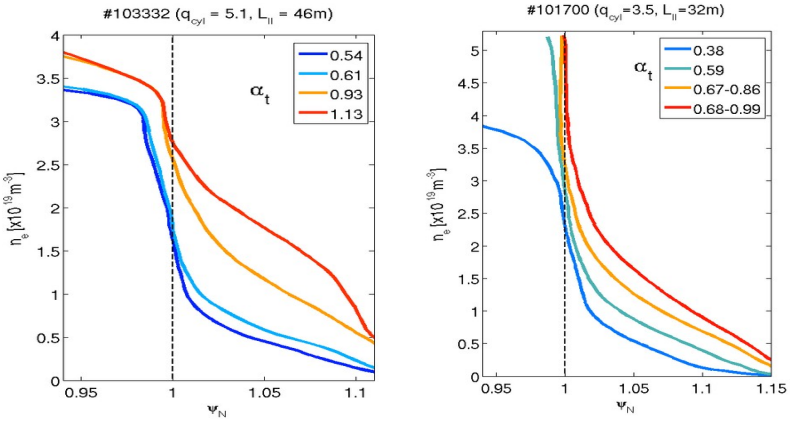

Figure 1: Density profile and α_t evolution during fuelling ramp up to H-L backtransition running same plasma shape at two different plasma currents (keeping Bt = 2.1T fixed): Ip =1.3MA (left) and Ip=1.9MA (right). Note the higher absolute values of density and lack of shoulder formation at 1.9MA.

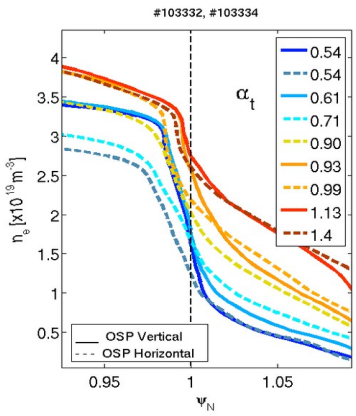

Figure 2: Comparison of edge density profiles over a wide range of α_t values, for two different OSP geometries (vertical or horiz. target).

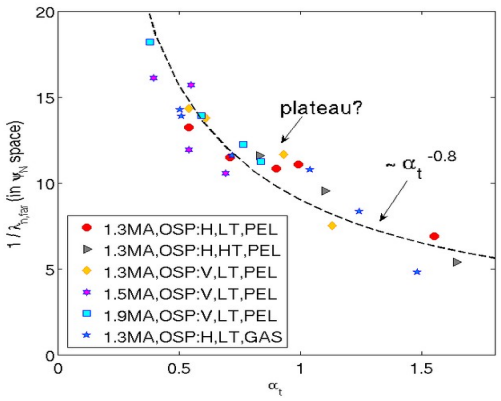

Figure 3: Density decay constant (=1/$\lambda_{n,far}$) in the far-SOL as a function of α_t for the full dataset of discharges. The legend provides additional information for each scenario (Ip, divertor geometry, low/high triangularity, fuelling method).

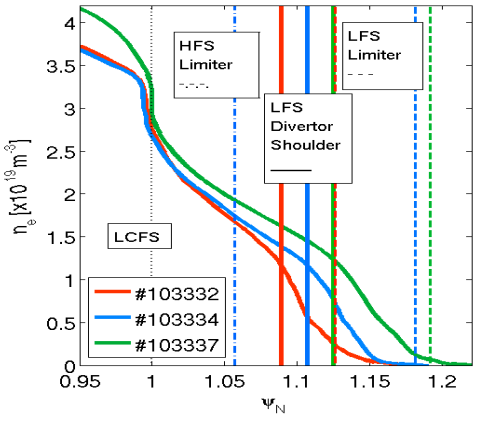

Figure 4: Density shoulders obtained with three plasma shapes, showing different outer inflection radii. The vertical lines (same colour convention as the profiles) mark the poloidal fluxes at which different wall parts are intersected.

References

[1] A Eksaeva et al 2022 Phys. Scr. 97 014001. [2] D. Carralero et al 2014 Nucl. Fusion 54 123005. [3] B. Tal et al Nucl. Fusion 64 (2024) 126063. [4] R.B. Morales *et al* RSI 95 (2024) 043501. [5] N. Vianello *et al* Nucl. Fusion 60 (2020) 016001. [6] T. Eich et al 2020 Nucl. Fusion 60 056016. [7] D. Carralero *et al* Nucl. Mat. Energy 12 (2017) 1189–1193. [8] Bernert M 2013 PhD Thesis LMU München (http://edoc.ub.uni-muenchen.de/16262/), page 52.